ChemComm

COMMUNICATION

View Article Online
View Journal | View Issue

Cite this: *Chem. Commun.*, 2015, **51**, 12305

Received 30th March 2015,
Accepted 29th June 2015

DOI: 10.1039/c5cc02623g

www.rsc.org/chemcomm

Water soluble, cyclometalated Pt(II)–Ln(III) conjugates towards novel bimodal imaging agents†

Oliver J. Stacey,[a] Angelo J. Amoroso,[a] James A. Platts,[a] Peter N. Horton,[b] Simon J. Coles,[b] David Lloyd,[c] Catrin F. Williams,[c] Anthony J. Hayes,[c] Jay J. Dunsford[d] and Simon J. A. Pope*[a]

Facile conjugation of a luminescent cyclometalated Pt^{II} complex with a DO3A-derived Gd^{III} moiety yields a hybrid species with visible luminescence and enhanced relaxivity.

A number of imaging techniques (MRI, CT, ultrasound, PET, SPECT, optical) are available at a biomedical level with various pros and cons for each regarding image resolution, depth of tissue penetration, acquisition time, and sensitivity. Therefore combining two or more imaging modalities into a single molecule agent can circumvent many limitations associated with a particular technique, whilst simplifying aspects of the agent administration and biodistribution characteristics (pharmacodynamics).[1]

It is very well known that trivalent lanthanide ions (Ln^{III}) offer remarkable opportunities in the design of biological imaging agents.[2] With dual applications in optical (luminescence)[3] and magnetic resonance imaging (MRI),[4] Ln^{III} complexes have been extensively studied and a range of ligand systems investigated. Therefore Ln^{III} moieties are particularly useful as a component of a bi- or multimodal single molecule imaging agent.[5] In this context, systems based on Gd^{III} have attracted most attention, with covalent coupling of organic fluorophores (MR/optical),[6] labelling with ^{18}F (MR/PET)[7] and ^{99m}Tc chelation (MR/SPECT)[8] providing prospective agents.

We are particularly interested in the use of phosphorescent metal-based luminophores[9] as components of dual MR/optical imaging agents. Such species offer distinct photophysical advantages (tunable emission wavelengths, large Stokes' shifts, long emission lifetimes) over fluorescent variants and can be very effective in cellular imaging studies using confocal fluorescence microscopy.[10] Cyclometalated Pt^{II} complexes can possess many of these beneficial luminescent properties and have been successfully applied to biological imaging.[11] In tandem with such physical attributes, interest in the use of Pt^{II} complexes with therapeutic benefits also continues.[12] Indeed one of the challenges of probing the (non)-specific biological action of Pt^{II} therapeutics often lies in the difficulty of directly imaging the biological action. In this context, Pt^{II} complexes can be tagged with fluorophores, such as anthraquinone, providing a means for identifying the intracellular fate of such compounds and understanding the role of targeting vectors.[13] Recent studies into Pt^{II} complexes of 2-phenylpyridine (ppy), have also explored binding with amyloid β peptide.[14] The influences of the Pt complexes on protein aggregation, *via* the inhibition of Cu and Zn peptide complex formation, have been suggested as an approach to the study of Alzheimer's disease.

In this work, we describe the development of water soluble Pt^{II}–Ln^{III} hybrid systems wherein the cyclometalated Pt^{II} moiety is luminescent. Previous work has described the synthesis of mixed Pt^{II}/Ln^{III} species and their photophysical properties, where the Pt^{II} chelate acts as an antenna for sensitised Ln^{III} emission within donor (Pt)–acceptor (Ln) assemblies.[15] However, such systems are often not water soluble or water stable, and thus, to the best of our knowledge, there are no reports on the water relaxometric properties of Pt^{II}–Gd^{III} heterometallic species. A number of other water stable d–f hybrids employing Ru^{II}, Re^{I} and Os^{II} as MLCT-based sensitisers have also been reported,[16] with Re^{I}/Ru^{II}–Gd^{III} hybrids demonstrating the physical properties for potential in dual MR/optical imaging.[17] The aim of this work was to synthesise a water-soluble Pt^{II}–Ln^{III} complex with favourable luminescence and relaxivity properties.

Two new ligands were required for the assembly of the Pt^{II}–Ln^{III} targets. Firstly, for the macrocyclic complex (**Ln–py**), a route was utilised[18] to give the ethylamine amide derivative (**P1**, ESI†), which subsequently reacted with 4-pyridinecarboxaldehyde using a reductive amination procedure (**P2**, ESI†);

[a] *School of Chemistry, Main Building, Cardiff University, Park Place, Cardiff, UK CF10 3AT. E-mail: popesj@cardiff.ac.uk; Tel: +44 02920 879316*
[b] *UK National Crystallographic Service, Chemistry, Faculty of Natural and Environmental Sciences, University of Southampton, Highfield, Southampton, UK SO17 1BJ*
[c] *School of Biosciences, Main Building, Cardiff University, Park Place, Cardiff, UK CF10 3AT*
[d] *School of Chemistry, The University of Manchester, Manchester, UK M13 9PL*

† Electronic supplementary information (ESI) available: All experimental and characterisation details, X-ray crystallographic data, TD-DFT, ^1H NMR spectra and ^1H NMRD plots. CCDC 1056166. For ESI and crystallographic data in CIF or other electronic format see DOI: 10.1039/c5cc02623g

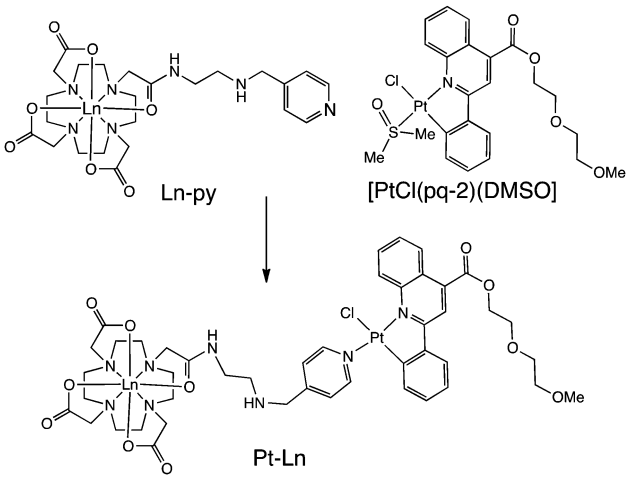

Scheme 1 Route to the heterometallic targets.

deprotection of the *tert*-butyl esters with trifluoroacetic acid and complexation with either $Gd(OTf)_3$ or $Yb(OTf)_3$ gave the monometallic Ln^{III} complexes, **Ln–py** (Scheme 1) possessing a pendant pyridine donor. Formation of the lanthanide complexes was confirmed by HRMS with additional ^1H NMR data for **Yb–py** (ESI,† Fig. S1) showing the pronounced chemical shifts of the azamacrocycle and arm protons between +135 and −80 ppm. For the hydrophilic Pt^{II} component, two 2-phenylquinoline derivatives incorporating a PEG-like functionality were synthesised, yielding both amide (**pq-1**, ESI†) and ester linked (**pq-2**, ESI†) derivatives from either 2-(2-aminoethoxy)ethanol or 2-(2-methoxyethoxy)ethanol, respectively.

The attempted synthesis of the Pt^{II} complexes was undertaken *via* the splitting of dimeric $[(L)Pt(\mu\text{-}Cl_2)Pt(L)]$ with DMSO to form the monometallic species [PtCl(**pq**)(DMSO)]. In our hands, the use of the hydroxyl terminated PEG derivative (**pq-1**) was not amenable to this synthetic pathway, giving a poor yield of the desired Pt^{II} complex. However, the methoxy analogue [PtCl(**pq-2**)(DMSO)], which would be expected to be slightly less hydrophilic than **pq-1**, was successfully isolated as an orange solid suggesting that the terminal hydroxyl group of **pq-1** may interfere with the coordination chemistry of Pt^{II}. [PtCl(**pq-2**)(DMSO)] was characterised *via* a range of techniques including $^{195}Pt\{^1H\}$ NMR which revealed a resonance at −3665 ppm. An X-ray crystal structure (Fig. 1) of [PtCl(**pq-2**)(DMSO)] was also obtained (crystal structure data and refinement parameters are contained in the ESI†) and revealed the anticipated coordination environment for Pt^{II}, with typical Pt–L bond lengths and angles for the coordinated atoms (ESI,† Table S1) and a distortion of *ca.* 7° in the phenylquinoline unit. The packing structure also revealed a head-to-toe arrangement, with some π-stacking between the phenylquinoline moieties; there are no intermolecular Pt–Pt interactions.

Finally, the two complexes **Ln–py** and [PtCl(**pq-2**)(DMSO)] were dissolved in a minimum volume of acetone and reacted at 40 °C for 48 h. The resultant **Pt–Ln** dimetallic complexes were obtained as extremely hygroscopic orange powders and the formation confirmed using HRMS (ESI,† Fig. S2), which revealed the distinct and appropriate isotopic distribution corresponding

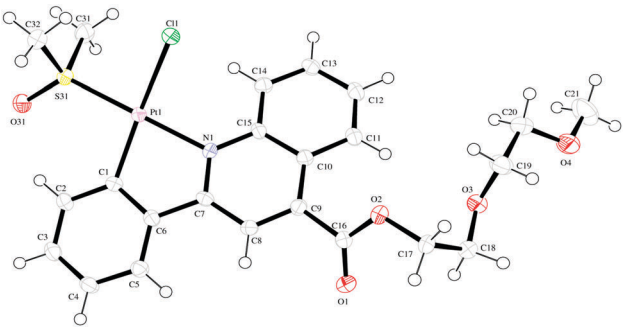

Fig. 1 X-ray crystal structure of [PtCl(**pq-2**)(DMSO)]. Probability of the ellipsoids is 50%.

to the loss of the chloride ligand to give the cationic dimer as $[M - Cl]^+$.

The electronic properties of [PtCl(**pq-2**)(DMSO)] show that the complex absorbs in the UV region, with $^1\pi$–π^* transitions associated with the phenylquinoline unit, and in the visible region with λ_{max} at 424 nm, which probably corresponds to a ^{1}MLCT type transition. Supporting theoretical (TD-DFT) calculations on the model complexes [PtCl(epqc)(DMSO)] (where epqc = 4-ethyl-2-phenylquinoline carboxylate) and [PtCl(epqc)(py)] (where py = pyridine) show that the majority of the electron density in the HOMO lies across both the phenyl moiety of the cyclometalated ligand and the 5d-orbitals of the platinum. The orbital representations of the calculated lowest energy HOMO–LUMO transitions are shown in the ESI,† (Fig. S3). The percentage contribution to the energy levels for the Pt^{II} 5d-orbitals (ESI,† Table S2) were calculated from the theoretical data showing that for both model complexes the HOMO comprises *ca.* 25% 5d-orbital character and is consistent, therefore, with a MLCT contribution.

The UV-vis spectra (Fig. 2) of the **Pt–Ln** hybrids are closely comparable to [PtCl(**pq-2**)(DMSO)], with the visible MLCT absorption characteristics retained for both **Pt–Gd** and **Pt–Yb**. The luminescence properties of [PtCl(**pq-2**)(DMSO)] revealed a broad, featureless emission band at 625 nm (λ_{ex} = 425 nm) with a corresponding lifetime of 116 ns, which are attributed to an excited state of triplet character which is likely to encompass a strong ^{3}MLCT component. The properties of the corresponding

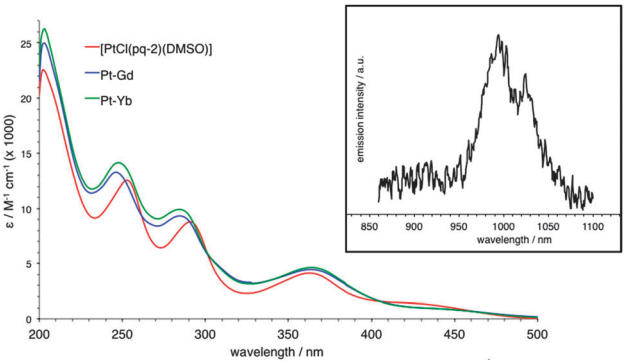

Fig. 2 Main: UV-vis absorption spectra of the complexes. Inset: Near-IR emission spectrum of **Pt–Yb** recorded in D_2O (λ_{ex} = 425 nm).

Table 1 UV-vis and luminescence properties of the complexes

Compound	λ_{abs}	λ_{em}/nm	τ/ns
[PtCl(**pq-2**)(DMSO)][a]	291, 362, 424	625[c]	116[e]
Pt–Gd[b]	285, 364, 426	617[c]	59[e]
Pt–Yb[b]	284, 364, 427	619,[c] 997[c,d]	50,[e] 902[d,f]

[a] $CHCl_3$ solution. [b] H_2O solution. [c] λ_{ex} = 425 nm. [d] Yb-based emission. [e] λ_{ex} = 372 nm. [f] λ_{ex} = 355 nm; λ_{em} = 975 nm.

Pt–Gd adduct were obtained in aqueous solution: the UV-vis spectrum shares all of the same features as [PtCl(**pq-2**)(DMSO)] with ^{1}MLCT absorption retained *ca.* 425 nm and visible luminescence observed at 617 nm (Table 1).

In comparison, the steady state luminescence spectrum (λ_{ex} = 425 nm) of **Pt–Yb** displayed dual emission comprised of ^{3}MLCT character at *ca.* 620 nm and Yb^{III} centred emission (inset, Fig. 2) in the near-IR region around 980 nm (corresponding to $^2F_{5/2} \rightarrow {}^2F_{7/2}$). Since absorption at 425 nm is dominated by the Pt^{II} chromophore this observation suggests that the Yb^{III} emission must be sensitised and therefore confirms the formation of the heterometallic dimer. For completeness, lifetime measurements on the donor component of the two **Pt–Ln** complexes were recorded in water to estimate the through-space Pt → Yb energy transfer rate, k_{ET}, (using $k_{ET} = (\tau_q)^{-1} - (\tau_{ref})^{-1}$ where τ_q is the ^{3}MLCT lifetime in the presence of Yb^{III} and τ_{ref} is the lifetime in the presence of Gd^{III}). The value for k_{ET} was calculated to be *ca.* 3×10^6 s^{-1}, which is similar to the rate of 2×10^6 s^{-1} for a previously reported Pt^{II}–Yb^{III} complex.[19]

The lifetimes of the Yb^{III} emission were also obtained in H_2O (0.90 μs) and D_2O (5.46 μs) to give an approximate inner sphere hydration ($q = k_{H_2O} - k_{D_2O} - 0.1$)[20] of 0.8, which is consistent with an octadentate Yb^{III} complex, implying that the amide carbonyl participates in the coordination sphere of Yb^{III}, as observed in related lanthanide complexes of mono-amide DO3A derivatives.[21]

The relaxivity properties of the Gd^{III} containing species were determined using field-cycling relaxometry. ^{1}H NMRD plots (ESI,† Fig. S4) were obtained for **Gd-py** and **Pt–Gd** (at field strengths between 1×10^{-2} – 30 MHz) to give bulk relaxivities, r_1, in water per mM of complex per second. The relaxivity of **Gd-py** was obtained as 3.8 mM^{-1} s^{-1} (30 MHz, 37 °C, pH 6.5), which is in accordance with the literature values for $[Gd(DOTA)(H_2O)]^-$, where r_1 was recorded as 3.8 mM^{-1} s^{-1} (20 MHz, 37 °C) and consistent with a q = 1 species.[22] Interestingly, the r_1 value for **Pt–Gd** was 7.1 mM^{-1} s^{-1} (30 MHz, 37 °C, pH 6.7), which shows that, upon formation of the dimetallic species, r_1 increases by 86%. This is most likely due to the increase in the molecular weight of the dimer resulting in a longer rotational correlation time, τ_R. The plots also demonstrate the temperature dependence of r_1 with relaxivities at 25 °C approximately 10–25% higher than at 37 °C (1×10^{-2} to 30 MHz).

Preliminary optical imaging studies were attempted with **Pt–Gd** using both MCF7 cells and *Schizosaccharomyces pombe* (fission yeast). Confocal fluorescence microscopy revealed that MCF7 cells poorly took up the complex with little evidence for internalisation. However, with *S. pombe* the images (ESI,† Fig. S5 and S6) clearly showed characteristic red emission from the cells, particularly those that were dividing, consistent with the Pt^{II}-based chromophore, showing that these species are compatible with confocal fluorescence microscopy.

Our studies have shown how a luminescent, amphiphilic cyclometalated Pt(II) chelate can be coupled with a macrocyclic hydrophilic Ln(III) species to give a water soluble dimetallic construct. Such an approach has allowed the study of heterometallic **Pt–Yb** and **Pt–Gd** species: sensitised Yb^{III} emission of the former corroborates the integrity of the dimer, while the latter reveals a bimetallic complex with visible luminescence properties and enhanced water relaxivity. Preliminary studies reveal that these complexes can be applied to the confocal fluorescence microscopy of cells, but that a careful balance of charge and amphiphilicity, and an understanding of cytotoxicity, will be required for future studies with different cell lines.

The EPSRC UK National Mass Spectrometry Facility (NMSF) at Swansea University, and the EPSRC UK National Crystallographic Service at the University of Southampton[23] are gratefully acknowledged.

Notes and references

1 L. E. Jennings and N. J. Long, *Chem. Commun.*, 2009, 3511; C. S. Bonnet and E. Toth, *C. R. Chim.*, 2010, **13**, 700; A. Louie, *Chem. Rev.*, 2010, **110**, 3146.
2 A. J. Amoroso and S. J. A. Pope, *Chem. Soc. Rev.*, 2015, DOI: 10.1039/C4CS00293H.
3 J.-C. G. Bunzli and C. Piguet, *Chem. Soc. Rev.*, 2005, **34**, 1048; C. P. Montgomery, B. S. Murray, E. J. New, R. Pal and D. Parker, *Acc. Chem. Res.*, 2009, **42**, 925.
4 C. F. G. C. Geraldes and S. Laurent, *Contrast Media Mol. Imaging*, 2009, **4**, 1; P. Caravan, J. J. Ellison, T. J. McMurry and R. B. Lauffer, *Chem. Rev.*, 1999, **99**, 2293.
5 For example, J. Luo, L.-F. Chen, P. Hu and Z.-N. Chen, *Inorg. Chem.*, 2014, **53**, 4184; J. Luo, W.-S. Li, L.-Y. Zhang and Z.-N. Chen, *Inorg. Chem.*, 2012, **51**, 9508.
6 C. Rivas, G. J. Stasiuk, J. Gallo, F. Minuzzi, G. A. Rutter and N. J. Long, *Inorg. Chem.*, 2013, **52**, 14284.
7 L. Frullano, C. Catana, T. Benner, A. D. Sherry and P. Caravan, *Angew. Chem., Int. Ed.*, 2010, **49**, 2382.
8 J.-A. Park, J. Y. Kim, H.-K. Kim, W. Lee, S. M. Lim, Y. Chang, T.-J. Kim and K. M. Kim, *ACS Med. Chem. Lett.*, 2012, **3**, 299.
9 R. G. Balasingham, F. L. Thorp-Greenwood, C. F. Williams, M. P. Coogan and S. J. A. Pope, *Inorg. Chem.*, 2012, **51**, 1419.
10 For example, A. J. Amoroso, R. J. Arthur, M. P. Coogan, J. B. Court, V. Fernandez-Moreira, A. J. Hayes, D. Lloyd, C. Millet and S. J. A. Pope, *New J. Chem.*, 2008, **32**, 1097.
11 For a comprehensive review: M. Mauro, A. Aliprandi, D. Septiadi, N. S. Kehr and L. De Cola, *Chem. Soc. Rev.*, 2014, **43**, 4144; S. W. Botchway, M. Charnley, J. W. Haycock, A. W. Parker, D. L. Rochester, J. A. Weinstein and J. A. G. Williams, *Proc. Natl. Acad. Sci. U.S.A.*, 2008, **105**, 16071.
12 K. D. Mjos and C. Orvig, *Chem. Rev.*, 2014, **114**, 4540; P. C. A. Bruijnincx and P. J. Sadler, *Curr. Opin. Chem. Biol.*, 2008, **12**, 197.
13 N. S. Bryce, J. Z. Zhang, R. M. Whan, N. Yamamoto and T. W. Hambley, *Chem. Commun.*, 2009, 2673; J. Z. Zhang, N. S. Bryce, A. Lanzirotti, C. K. J. Chen, D. Paterson, M. D. de Jonge, D. L. Howard and T. W. Hambley, *Metallomics*, 2012, **4**, 1209; E. E. Langdon-Jones and S. J. A. Pope, *Coord. Chem. Rev.*, 2014, **269**, 32.
14 F. Collin, I. Sasaki, H. Eury, P. Faller and C. Hureau, *Chem. Commun.*, 2013, **49**, 2130.
15 N. M. Shavaleev, P. P. Moorcraft, S. J. A. Pope, Z. R. Bell, S. Faulkner and M. D. Ward, *Chem. – Eur. J.*, 2003, **9**, 5283.
16 S. J. A. Pope, B. J. Coe, S. Faulkner and R. H. Laye, *Dalton Trans.*, 2005, 1482.

17 T. Koullourou, L. S. Natrajan, H. Bhavsar, S. J. A. Pope, J. Feng, J. Narvainen, R. Shaw, E. Scales, R. Kauppinen, A. M. Kenwright and S. Faulkner, *J. Am. Chem. Soc.*, 2008, **130**, 2178; G. Dehaen, P. Verwilst, S. V. Eliseeva, S. Laurent, L. V. Elst, R. N. Muller, W. M. De Borggraeve, K. Binnemans and T. N. Parac-Vogt, *Inorg. Chem.*, 2011, **50**, 10005.
18 S. G. Crich, D. Alberti, I. Szabo, S. Aime and K. Djanashvili, *Angew. Chem., Int. Ed.*, 2013, **52**, 1161; J. P. Andre, C. Geraldes, J. A. Martins, A. E. Merbach, M. I. M. Prata, A. C. Santos, J. J. P. de Lima and E. Toth, *Chem. – Eur. J.*, 2004, **10**, 5804.
19 T. K. Ronson, T. Lazarides, H. Adams, S. J. A. Pope, D. Sykes, S. Faulkner, S. J. Coles, M. B. Hursthouse, W. Clegg, R. W. Harrington and M. D. Ward, *Chem. – Eur. J.*, 2006, **12**, 9299.
20 A. Beeby, I. M. Clarkson, R. S. Dickins, S. Faulkner, D. Parker, L. Royle, A. S. de Sousa, J. A. G. Williams and M. Woods, *J. Chem. Soc., Perkin Trans. 2*, 1999, 493.
21 J. E. Jones, R. L. Jenkins, R. S. Hicks, A. J. Hallett and S. J. A. Pope, *Dalton Trans.*, 2012, **41**, 10372.
22 J. Costa, E. Toth, L. Helm and A. E. Merbach, *Inorg. Chem.*, 2005, **44**, 4747.
23 S. J. Coles and P. A. Gale, *Chem. Sci.*, 2012, **3**, 683.